



Metrology inside a cryostat using a cutting-edge periscope

Adrien Girardot, Jean-Emmanuel Migniau, Edgard Renault, Magali Loupiau,
Aurélien Jarno, Alban Remillieux

► To cite this version:

Adrien Girardot, Jean-Emmanuel Migniau, Edgard Renault, Magali Loupiau, Aurélien Jarno, et al.. Metrology inside a cryostat using a cutting-edge periscope. SPIE Optical Metrology 2023, SPIE, Jun 2023, Munich, Germany. pp.126180J, <10.1117/12.2673663>. <hal-04193638>

HAL Id: hal-04193638

<https://hal.science/hal-04193638v1>

Submitted on 1 Sep 2023

HAL is a multi-disciplinary open access archive for the deposit and dissemination of scientific research documents, whether they are published or not. The documents may come from teaching and research institutions in France or abroad, or from public or private research centers.

L'archive ouverte pluridisciplinaire **HAL**, est destinée au dépôt et à la diffusion de documents scientifiques de niveau recherche, publiés ou non, émanant des établissements d'enseignement et de recherche français ou étrangers, des laboratoires publics ou privés.



Distributed under a Creative Commons CC BY 4.0 - Attribution - International License

Metrology inside a cryostat using a cutting-edge periscope

Adrien Girardot^a, Jean-Emmanuel Migniau^a, Edgard Renault^b, Magali Loupiau^a, Aurélien Jarno^a, and Alban Remillieux^a

^aUniv Lyon, Univ Lyon1, Ens de Lyon, CNRS, Centre de Recherche Astrophysique de Lyon
UMR5574, F-69230, Saint-Genis-Laval, France

^bAix Marseille Univ, CNRS, CNES, LAM, Marseille, France

ABSTRACT

The PIC (Photogrammetry Inside Cryostat) is a cutting-edge periscope designed to be used during the prototyping, testing and alignment phase of HARMONI, one of the first-generation instruments of the Extremely Large Telescope. The challenge posed by operating the HARMONI instrument at a temperature of 130 K required the development of different non-contact measurement techniques to qualify optical and mechanical parts without touching them. Photogrammetry is a non-contact measurement technique, but it needed to be adapted to be used in a cryostat ; this led to the development of the PIC. The periscope consists of a combination of six lenses, two mirrors, and three motorized degrees of freedom (the whole is mounted upside down on the lid of the test cryostat at CRAL in Lyon) and work together with an external camera to capture images at various angles. This is essential for obtaining accurate photogrammetric measurements. The motorized rotation systems allow for precise and controlled movements, and the combination of lenses and mirrors ensure that the images captured by the external camera are of the highest quality. The goal of the PIC is to obtain an accuracy of $25 \mu m + 5 \mu m/m$, making it an essential component of the HARMONI tools and a major advancement in cryogenic photogrammetry.

Keywords: Photogrammetry, Metrology, Periscope, 3D reconstruction, HARMONI, ELT

1. INTRODUCTION

High Angular Resolution Monolithic Optical and Near-infrared Integral field spectrograph or HARMONI [1], [2] is one of the first-generation instruments of the Extremely Large Telescope (ELT). HARMONI capture the light that goes through the ELT and process it with an adaptive optics system. Then, the light enters a cryostat (named IFS for Integral Field Spectrograph). Among other sub-systems, the Integral Field Unit (IFU)^[3] slices the image to create a slit that is then used to feed the spectrographs. The IFS operates at a temperature of 130 K. To qualify optical and mechanical parts, different non-contact measurement techniques need to be developed. Among these techniques, photogrammetry emerged as a potential solution, but its use in cryogenic conditions posed significant challenges. To adapt photogrammetry in a cryogenic environment, it is necessary to take pictures inside the cryostat. As a result, we developed the Photogrammetry Inside Cryostat tool (PIC): a cutting-edge periscope that combines six lenses, two mirrors, and three motorized degrees of freedom. The PIC enables the capture of images from different angles all around any object placed inside the CRAL's test cryostat to obtain accurate photogrammetric measurements. As a reference, we use a commercial photogrammetric system. This system can reach a accuracy of $2 \mu m + 5 \mu m/m$ (RMS) and we will try to stay as close as possible to this value. This article discusses the development of the PIC and its application during the prototyping, testing, and alignment phase of the HARMONI instrument. In section 2, we will present the periscope and its specifications. Then, the section 3 addresses the alignment of the system. The section 4 is dedicated to the qualification procedure of the periscope. Then, in section 5, we will present an evaluation of the photogrammetric accuracy. Finally, we will talk about the PIC's application for the AIT phase of HARMONI.

Further author information:

Adrien Girardot.: E-mail: adrien.girardot@univ-lyon1.fr, Telephone: +33 7 83 59 63 32

2. CHARACTERISTICS OF THE PERISCOPE

In this section, we will delve into the specifications and design of the periscope, including the optical design and mechanical design that make it a functional tool to perform photogrammetry.

2.1 Specifications

The periscope-based optical system is designed to overcome spatial constraints within the CRAL's cryostat, which has a diameter of 1 meter and a height of 700 mm. To accommodate these limitations, the decision was made to position the camera externally, fixed behind a porthole of the cryostat. The periscope is equipped with three motorized degrees of freedom to facilitate precise and controlled movements. The first degree of freedom (R1) enables a 360-degree rotation, allowing for comprehensive viewing angles of the test piece. The second degree of freedom (R2) allows the periscope to dive inside the cryostat, while the third degree of freedom (R3) enables scanning of most of the cryostat's volume. The periscope specifications include an object field of view of at least 45 degrees, ensuring the capture of a significant portion of the scene in each picture. It should have a depth of field of approximately 200 mm, providing adequate measurement capabilities for objects inside the test cryostat. The periscope must be vacuum compliant, capable of withstanding a pressure of 10^{-5} mbar, and weight less than 15 kg. It is fixed upside down on the lid of the cryostat, and hence stays at room temperature. To mitigate radiation interference, a Multi-Layer Insulation cover will be used to insulate the periscope. Maintaining excellent image quality is of paramount importance. Therefore, the periscope's specifications dictates a spot radius limit of seven pixels and a maximum distortion less than 0.1%. These specifications, along with additional details, are provided in Table 1 to offer a comprehensive understanding of the periscope's capabilities.

Size	Ø 1m, 700 mm height
Working temperature	293 K
Vacuum compliant	10^{-5} mbar of pressure
Motion	3 degrees of freedom : 1st rotation (R1) : 360 degrees 2nd rotation (R2) : 30 degrees 3rd rotation (R3) : 70 degrees
Mass	$\leq 15kg$
Fixation	fixed upside down on the lid of the cryostat
Depth of field	$\approx 200mm$
Field of view	200 mm in object plane (40°)
Image quality	Spot radius $\leq 7pixels$
Distortion	$\leq 0.1\%$
Focal length equivalent	1000 mm $\pm 1\%$
Wavelength	Visible

Table 1: Specifications of the periscope.

2.2 Opto-mechanical design

This section will outline the PIC's optical design, which works in combination with three motorized degrees of freedom. Additionally, it will cover the design of the barrels used to house the lenses and mirrors.

2.2.1 Optical design

The Photogrammetry Inside Cryostat (PIC) utilizes an optical design consisting of 6 single lenses, a parallel plate, and 2 flat mirrors. The design takes into consideration the operating environment within the cryostat, requiring the system to operate in a high vacuum environment (around 10^{-5} mbar). To avoid outgassing of optical glue, the decision was made to employ only single lenses. The PIC is designed to provide an image at infinity, with the exit pupil positioned 20 mm above the window. It is paired with a macro lens, specifically the Nikon AF-S 60mm micro $f/2.8$ G ED, known for its excellent image quality and low distortion characteristics. The lens is used with a distance ring set to infinity. Due to the unknown position of the entrance pupil of the

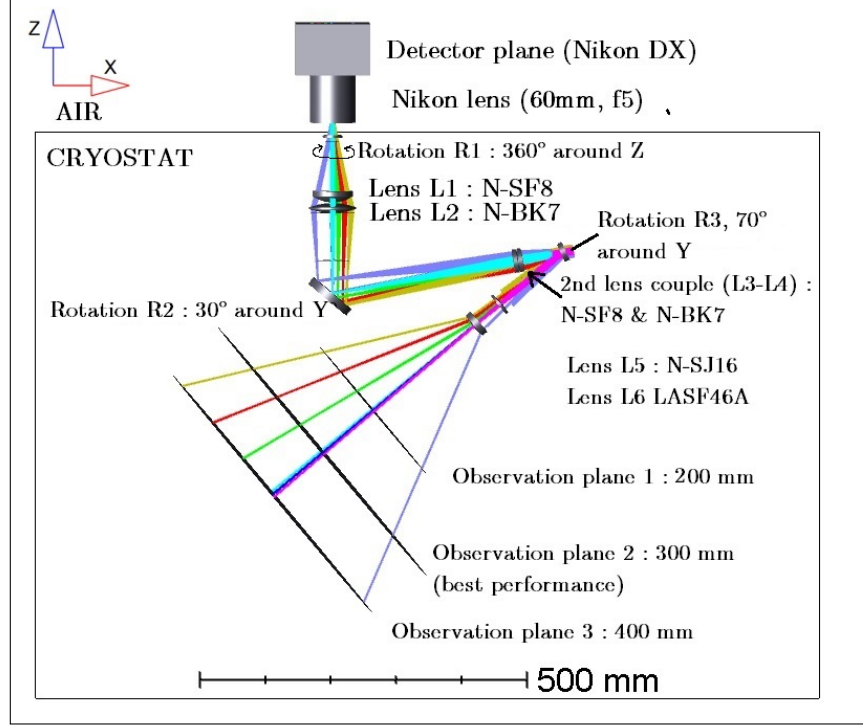


Figure 1: Zemax shaded model

lens, the lens+detector assembly can be translated along the optical axis to align the exit pupil of the PIC with the entrance pupil of the Nikon lens. With a focal length of 1000 mm, the PIC achieves a magnification of 16.66 when used in conjunction with the Nikon lens. This results in an image field of view of $\pm 12^\circ$ on a DX $24 \times 16 \text{ mm}$ camera sensor with a $4 \mu\text{m}$ pixel size, while the object field of view obtained is $\pm 218 \text{ mm}$. The $4 \mu\text{m}$ pixel size in image space corresponds to $64 \mu\text{m}$ in object space. In order to minimize manufacturing costs, conventional lenses were chosen for the design, and the radii of curvature were determined in collaboration with the lens manufacturer to utilize their existing manufacturing calibres (lens calibration).

2.2.2 Design of the barrels

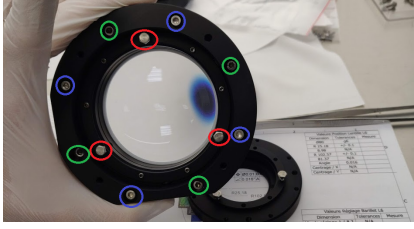
To ensure that a good alignment is reachable, each lens is on a different barrel. Each barrel can be adjusted in tip/tilt. Furthermore, on each doublet (L1-L2, L3-L4 or L5-L6), one of the barrels has two translation stages. By using these translations, it is possible to align both lenses on the same optical axis and keep both of the barrel co-linear by doing the procedure describe in Sec. 3.1. This is mandatory because each doublet is then mounted on the same tube and this constrains the co-linearity between the two barrels. Then, each tube will be mounted using eccentrics ($\pm 1 \text{ mm}$) to place each doublet on the optical axis.

2.3 Design of the rotations

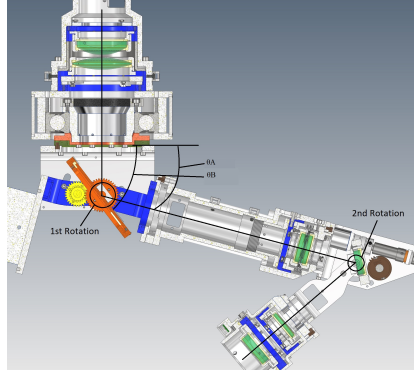
The optical beam is oriented by the way of two mirrors M1 and M2 (see Fig. 4). To follow the refraction law, the mirror rotates of θ_B implies the θ_A , rotation of the next tube, is following :

$$\theta_A = 2 \times \theta_B \quad (1)$$

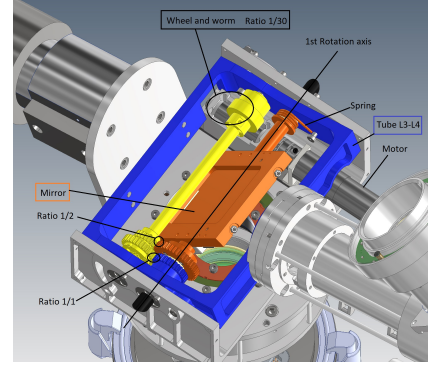
In order to stabilise the system during the shooting, we used the wheel and worm principle (Fig. 2c). When the PIC reaches the appropriate value, the motor can stay off. The wheel drives the mirror and the tube L3-L4 (represented in blue in Figs. 2b & 2c) with two different ratios (1/1 and 1/2). The mirror stays in contact with the tube L3-L4 thanks to the spring. In this way, there is no play during the rotation. And finally, the mirror and the tube turned around the rotation axis according to the alignment plan. The geometry of the wheel and worm allow the system to have a mechanical accuracy of 43 arcseconds.



(a) Red: tilt adjustment. Blue: translation along X. Green: translation along Y



(b) First rotation (R1)



(c) Details of transmission for R1

Figure 2: Mechanical design of the PIC

3. INTEGRATION AND ALIGNMENT

In this part, we will explain the alignment procedure of the periscope. The alignment was a key step to ensure the accuracy of the photogrammetric measurement. The alignment is divided in two milestones : an alignment on line (without the outside mechanical parts and mirrors) and the alignment once the periscope is fully assembled. We will firstly present the on-line alignment.

3.1 On-line optical alignment

Firstly, we integrated the lenses on their barrels. As presented on Fig. 2a, each lens has its tip/tilt adjustments. Once all the lenses are integrated, we define an optical axis using a laser beam. The optical axis is set parallel to the table. Then, all the lenses are aligned on this optical axis one after the other (see Fig. 3 top). The alignment is set by autocollimation using the return signal on each face of the lenses. Once the lenses are aligned, the goal was to set the barrels of each doublet to be co-linear. To do so, we moved the barrel that has the XY translation (cf Sect. 2.2.2) to align it with the other barrel and then translated the lens (using the XY translation) to its initial position. Afterwards, the lenses are integrated on the tubes (Fig 3 bottom). There is one tube for each doublet (represented in red on Fig. 4). After this, another alignment must be done. The laser beam still defines the optical axis and the goal was to align the tubes on this optical axis. There were 4 adjustments for each tube : X, Y, θX and θY . Autocollimation was also used here. Once the alignment was made, we performed

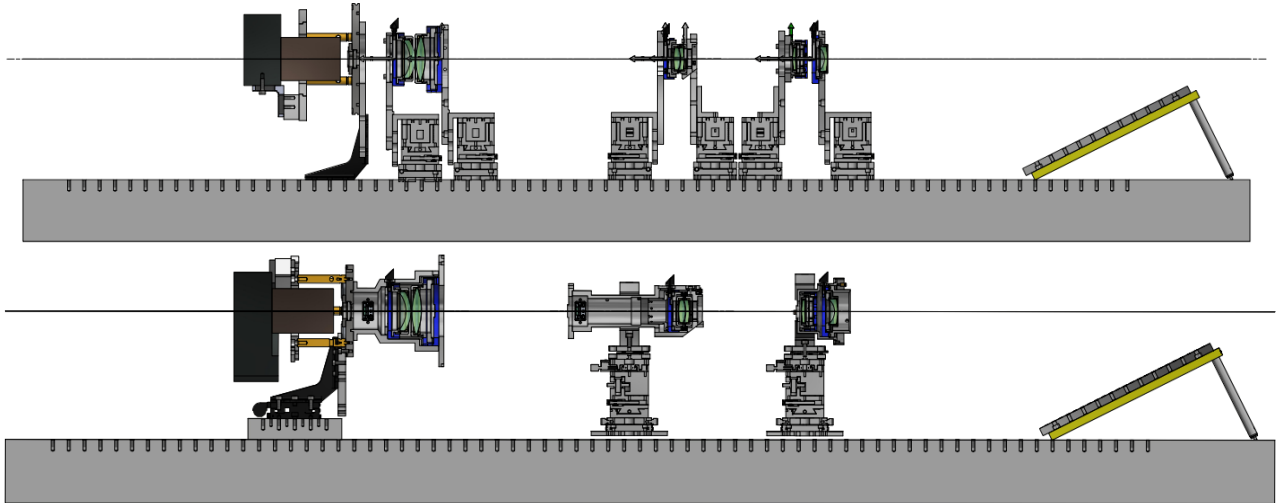


Figure 3: The two steps for the on-line alignment of the periscope

a mechanical measurement using a 6-axis metrological arm. The goal of this measurement was to control the positions of the tubes and check if it was compatible with the next steps of the assembly. They must be placed within 1 mm in X and Y (which corresponds to the eccentric's dynamic), and within 0.04 degrees. The measured parameters are presented on table 2. On this table, we can see that the elements have been aligned within the tolerance. The tubes are on the range of the eccentrics and the angles are small enough to keep the optical quality intact. We use this step of the alignment to align the removable mirrors m1, m2 and m3 (purple mirrors on fig 4) on the optical axis using autocollimation. These mirrors will be used as references during the alignment because they represents the optical axis on which the lenses has been aligned at this step. At this point, the image quality is quantified as describe in Sec. 4.

Barrel	L1-L2	L3-L4	L5-L6	specs
X(mm)	-0.01	0.10	0.02	1.00
Y(mm)	0.01	0.11	-0.10	1.00
$\theta X (^{\circ})$	-90.01	-89.99	90.03	0.04
$\theta Y (^{\circ})$	-180.00	179.99	-0.02	0.04

Table 2: On-line alignment report. XY translation must be within $\pm 1 \text{ mm}$. θ must be within $\pm 0.04^{\circ}$

3.2 Complete assembly and final alignment

Now that the on line alignment of all of the barrels is compliant, we can fully assemble the PIC. The next step was to align the periscope. To make a correct alignment, we needed to adjust 14 parameters : 10 translations and 4 tilts. The translations are represented by the eccentrics at the interface of each parts (in orange on Fig. 4) and the tilts adjustments are the angles of the 2 mirrors of the periscope (in green on the scheme) and the tilts of the laser beam. First, we aligned the target to the center of the bearing using its barrel and the camera. Then, we aligned the laser on the L1-L2 tube with the XY0 tilt and translation to center the beam on the target. Afterwards, we used the autocollimation on m2 to align M1 ($\theta 1$). Next, we aligned the L3L4 tube with the XY2 translation using the bearing and target rotation. The beam should remain in the center of the target. Then we used the autocollimation on m3 to align M2 ($\theta 2$). Next, we aligned the $\theta 2$ axis with the Y3 translation and m3 using the bearing and target rotation. The beam should remain in the center of the target. Finally, we align L5-L6 with the XY4 translation. It must be centered.

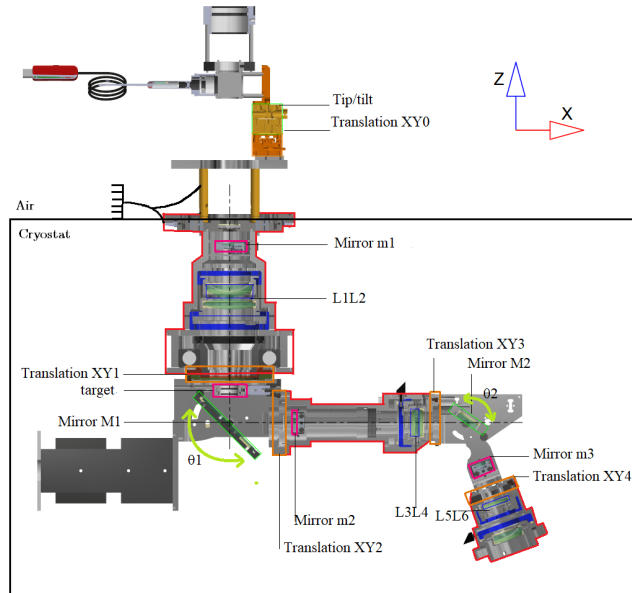


Figure 4: Convention for the alignment. Red : tubes that contains two lenses. Orange : XY eccentrics translations. Green : mirrors. Purple : alignment mirrors or target, removable

4. QUALIFICATION PROCEDURE

This section, explains the validation procedure that allows us to monitor the image quality of the periscope. We will detail the MTF (Modulation Transfer Function) measurement of the periscope.

4.1 MTF measurement.

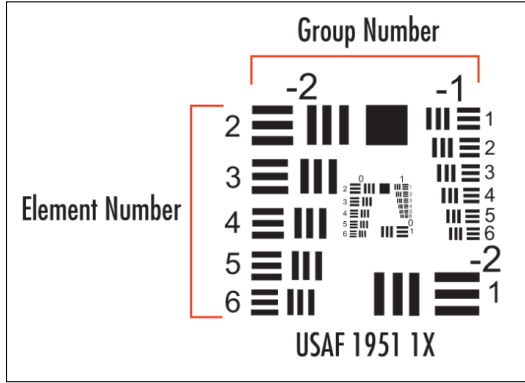
To measure the MTF, we use an USAF-1951 target (as shown in Fig. 5a). The USAF target is place in the focal plane of the periscope and we capture an image of this target. Each series of bars corresponds to a resolution. This resolution can be calculated using formula (1), where R is the resolution expressed in line pairs per millimeters.

$$R = 2^{Groupe\ number + \frac{Element\ number - 1}{6}} \quad (2)$$

The contrast is then calculated for each series of three bars using the formula:

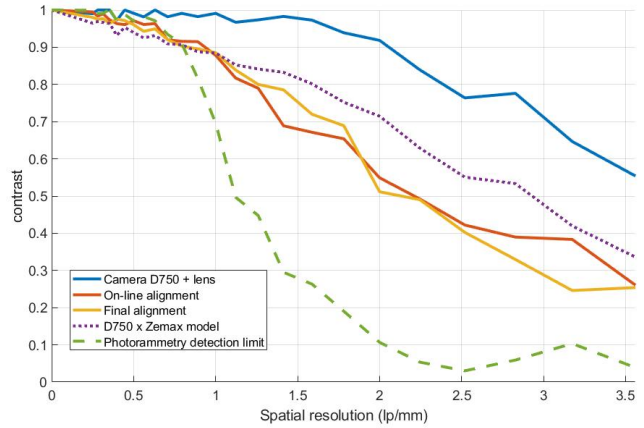
$$C = \frac{L_{max} - L_{min}}{L_{max} + L_{min}} \quad (3)$$

Therefore, we can plot the contrast (C) with respect to the resolution (R). Results are presented on Fig. 5b. On this figure, we can compare the image quality of the PIC after the in-line alignment (yellow curve) and after the complete assembly (red curve). The top blue curve corresponds to the MTF of the camera alone, and the bottom dash-line curve is the limit MTF under which a measurement by photogrammetry is impossible. Finally, the top dash curve corresponds to the product of the D750 MTF plus objective and the PIC MTF computed by Zemax. This curve is the theoretical curve if the alignment is perfect. This shows that the fully-assembled alignment has been made without degrading the image quality of the on-line alignment and that we are 10% below the theoretical value.



(a) MTf USAF1951 target.

Source : www.edmundoptics.com



(b) MTF computed for the PIC in various configurations

Figure 5: Image quality evaluation using MTF

5. EVALUATION OF THE PHOTOGRAMMETRIC ACCURACY

Now that the periscope is assembled and that the MTF is compliant with the specification, it is important to check if the photogrammetric measurement is in the specification.

5.1 The measurement protocol

To do so, we mounted a test scene. This scene is composed of two reference bars in Zerodur (in blue on Fig.6a), 25 coded targets to orient each image (in red), and a translation stage with 4 targets on it (yellow). Using the PIC, we take several pictures (around eighty) all around the scene and with different viewing angles. Then, these pictures are used by the software to compute the position of each target in space. The software also estimates the defaults of the camera (the periscope here), and adjust these parameters to retrieve the positions of the targets. The parameters that the software adjusts are :

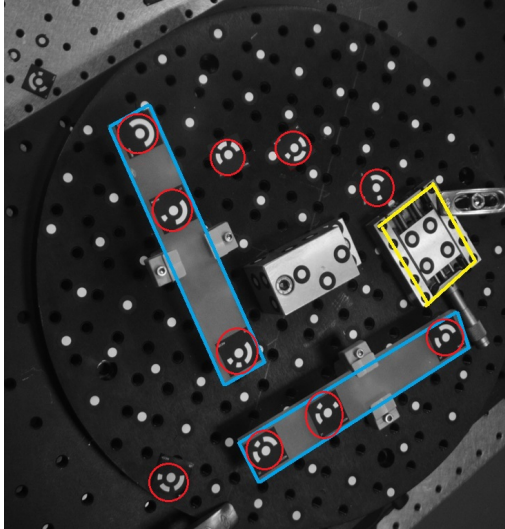
- 📷 Focal length
- 📷 XH, YH : Coordinates of the principal point
- 📷 A1, A2, A3 : Coefficients of the radial distortion polynomial.
- 📷 B1, B2 : Coefficients of the tangential distortion polynomial.
- 📷 C1, C2 : Affine transformation (sensor orthogonality) and scaling.

Then, we can compare a first measurement with the PIC with another measurement of the same scene but with the translation stage moved of $50\text{ }\mu\text{m}$. This allows us to see if a movement of 50 microns is perceptible or overwhelmed in the noise.

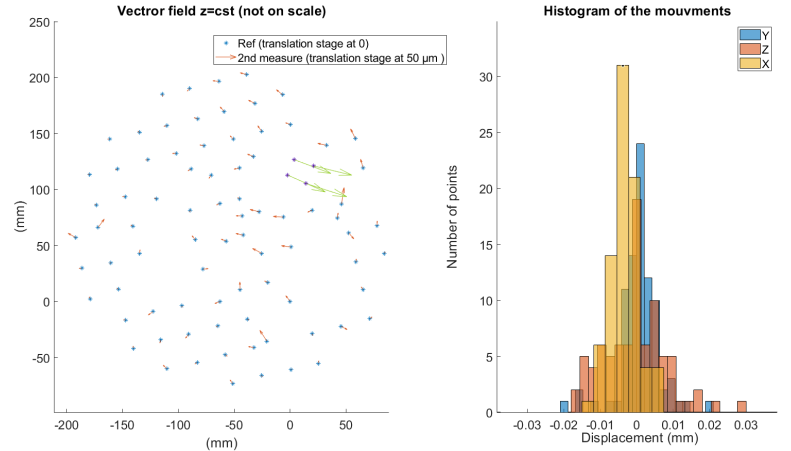
5.2 Motionless PIC

Firstly, we made this measurement with the PIC in only one position and the scene is moving. In this configuration, the alignment is the same in all the pictures (because the PIC is not moving). Figure 6b represent the movement of each target between the two measurements. We can clearly see where are the four targets that has been moved of 50 microns. The histograms allows us to reach two conclusions :

- In this ideal case, a movement of 50 microns is clearly identifiable.
- The limit of precision of the PIC is at 10 microns in this ideal configuration (define by the Gaussian in Fig 6b).



(a) Scene used to qualify the periscope



(b) Displacement between the two measurements with the PIC fixed in one position (the scene is moving). The green arrows are the movement of the translation stage between the two measurements.

Figure 6: Evaluation of the photogrammetric accuracy

5.3 Moving PIC : single calibration

The next step is to find a procedure that allows to reach the same accuracy with the PIC moving. 2 methods are considered here : A global adjustment of the parameters of the camera (i.e. the mean of each parameters in every positions of the PIC) or an adjustment for each position of the periscope. Here, we will present the first method of calibration because it is the simpler. We take around 80 pictures with the PIC moving all around the scene. The alignment could not be absolutely stable (regardless our efforts) in all the periscope positions. For this reason, the software will compute a mean value for all the parameters presented above. Using these images, we tried the same measure as presented Fig. 6b with a $50 \mu\text{m}$ displacement but this displacement is at the edge of the noise (see Fig. 7). To improve this accuracy, we have to find a way to calibrate each position of the periscope. To do so, the next part will be dedicated to the study of the variation of these parameters with respect to the movement of the PIC.

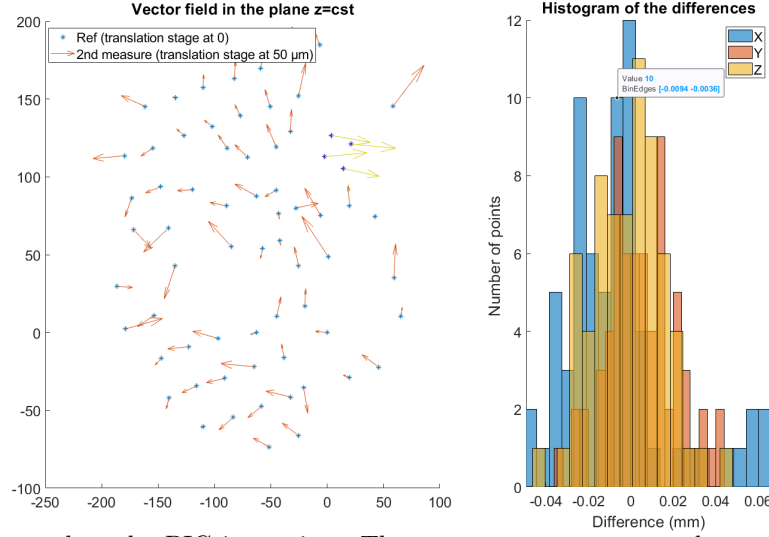


Figure 7: Measurements when the PIC is moving. The green arrows corresponds to the displacement we are trying to see.

5.4 Moving PIC : multiple calibrations

As said in part 5.1, the software allows us to calibrate the camera using several parameters. In this section, we will study the stability of these parameters according to the rotations of the periscope.

5.4.1 Study of the calibration parameters

To do so, we made 9 different calibrations in 9 different positions of the R1 rotation (see Fig. 8a). Then, we trace the evolution of the calibration parameters with respect to the angle of R1. In this procedure, A3 and C1 and C2 are set to 0 to reduce the number of parameters. Finally, we made another set of measurements after moving and repositioning the motors at the same position to study the repeatability. These measurements are marked in red. Figure 8b shows the evolution (A for the first position and J for the last one) of the coordinate of the principal point in image space coordinates. The tangential distortion parameters B1 and B2 (Fig. ??) seems to be very stable. A simple sine gives a R^2 of 0.9986. This curve is of the form of :

$$f(x) = a_0 + a_1 \times \cos(\theta \times \omega) + b_1 \times \sin(\theta \times \omega) \quad (4)$$

This means that anywhere between the measured points, we are confident that the parameters will be close to the one on the curve. Furthermore, this coefficient seems to be stable because the red points are really close to the coloured ones. For the tangential distortion coefficients, this is less straightforward (Fig. 8c). The points do not align on a sine curve or any *simple* curve with an R^2 greater than 0.99. In addition, the repeatability test gives points that are quite far compare to B1 & B2. We then conducted the same measurements with the

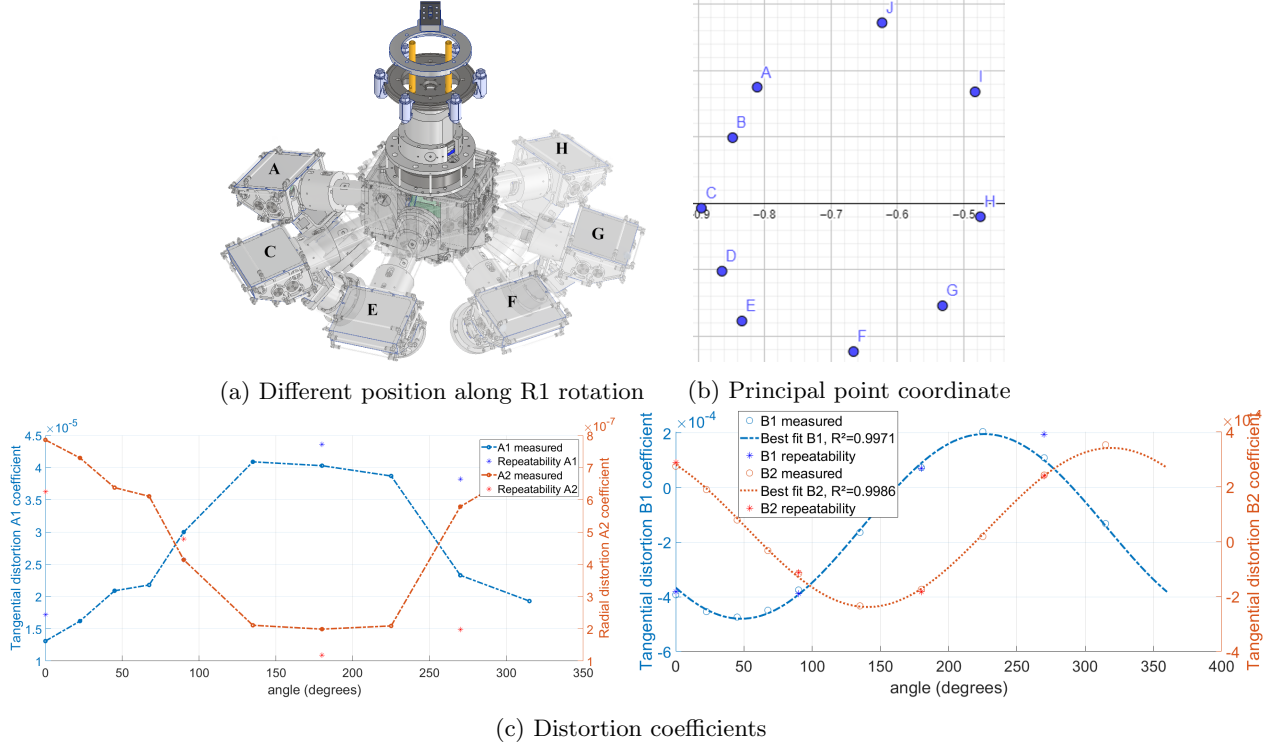


Figure 8: Evolution of the camera calibration parameters with respect to the rotation of R1.

other two rotations. These measurements show that the amplitude of the evolution of the distortion parameters is much smaller than the one induce by R1 ($\approx 5\%$). Based on this finding, we can disregard the impact of the other two rotations on the camera parameters. Consequently, the calibration parameters solely rely on the periscope's position around the R1 rotation.

5.4.2 Prediction of the camera parameters.

Using the curves Fig. 8, the calibration parameters can be predictable. Using this, as in Sec. 5.1, we made 2 measurements : one as a reference and another with the translation stage 100 microns further. The results are

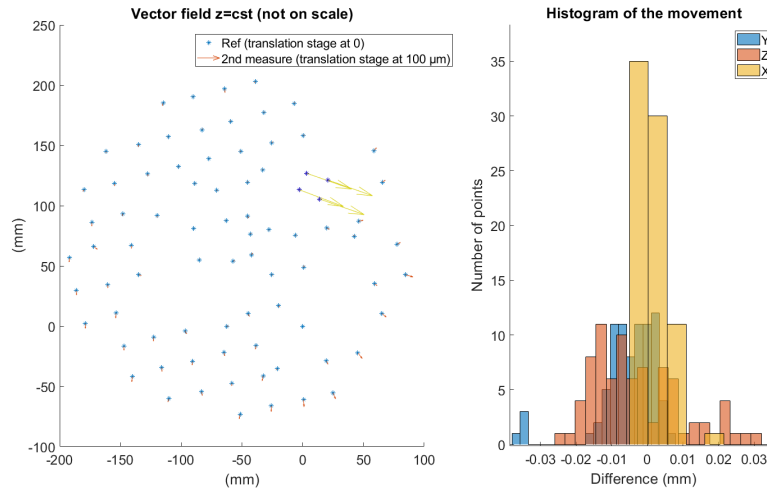
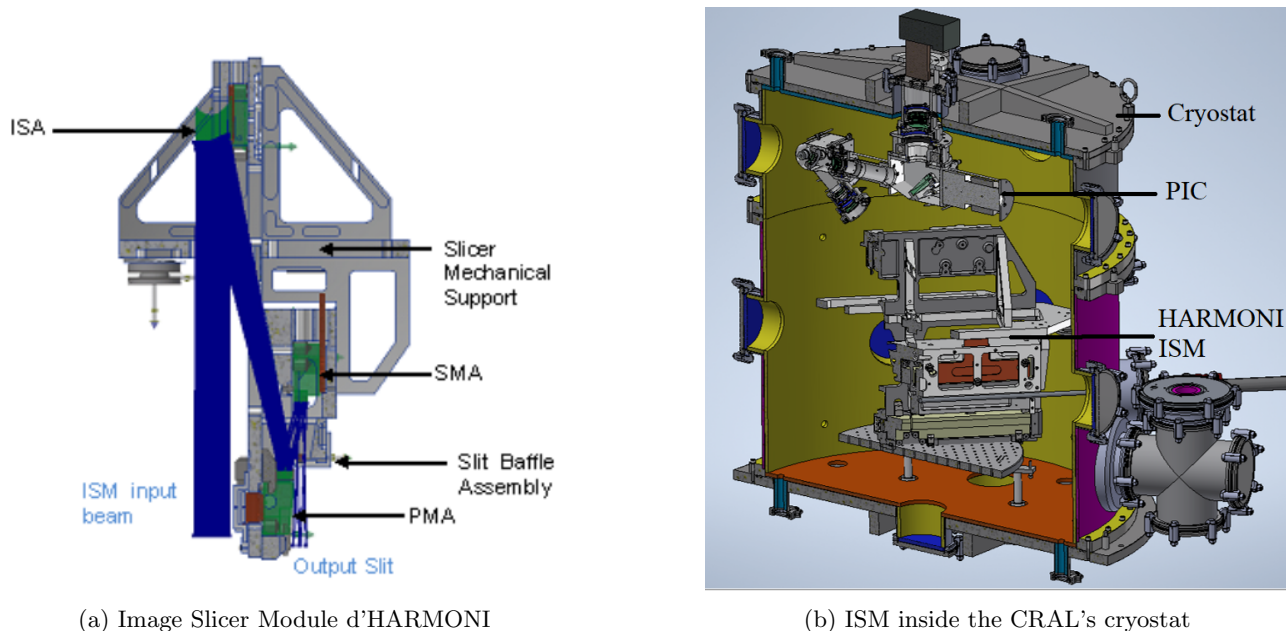


Figure 9: Displacement between the two measurements with the moving PIC for a 100 microns translation movement.

plots on Fig. 9. This measure shows that we can reach an accuracy of 20 microns with the moving periscope. Thus, we have demonstrated the usefulness of camera calibration in reducing uncertainty by half. A deeper study can reduce this accuracy to reach the one of the motionless PIC.

6. APPLICATIONS ON THE AIT PHASE OF HARMONI

This part will be a discussion about the possible cases of application of the PIC during the AIT phase of HARMONI. The CRAL team is in charge of delivering the Integral Field Unit (IFU) for HARMONI [3] to the institute assembling the full Integral Field Spectrograph in UKATC in Edinburgh. This sub-system is composed of mirrors only and has the function to slice the input rectangular field of view into 4 pseudo slits to feed 4 spectrographs. The Integral Field Unit is composed of two main optical modules, namely the Splitting and Relay Module (SRM) and Image Slicer Module (ISM) (Fig. 10a) together with a structural module called IFU Main Structure (IMS). The mirror substrate are Zerodur or silica and their mounts are made up of aluminium.



(a) Image Slicer Module d'HARMONI

(b) ISM inside the CRAL's cryostat

Figure 10: Metrology for the HARMONI ISM

Several kinds of mounts have been developed in CRAL[4], adjustable, blocked systems or shimmed systems. The tolerance analysis of the sub-system has been assessed using position measurement accuracy of $20\ \mu\text{m}$. The goal of the PIC is to reach this accuracy in a cryogenic environment and check that our mounts behave as expected. The ISM is the critical module of the sub-system and will be fully tested inside the cryostat (see Fig. 10b). The PIC will be to validate the displacement of the optical elements are as expected within a few mm to $20\ \mu\text{m}$ accuracy.

7. CONCLUSION

In conclusion, the development of the PIC periscope has been a major advancement in the field of cryogenic photogrammetry. Its use within the cryostat for the HARMONI project has successfully addressed the challenge of accurately measuring optical and mechanical components without physical contact, in a constrained environment such as CRAL's cryostat. The results obtained have demonstrated that the PIC periscope is capable of achieving an accuracy of 15 microns under ideal conditions when the periscope remains stationary. However, maintaining the same level of precision becomes more challenging during periscope movements, with maximum values reaching 20 microns. Moving forward, it is crucial to continue exploring the camera calibration parameters. Our next objective is to install the periscope inside the cryostat and assess its performance in a vacuum. Previous studies on prototypes have indicated that the optical quality of the periscope is not degraded by the

vacuum environment. Furthermore, it will stay at room temperature even when the cryostat is cool down. This research will contribute to increasing measurement precision and maximizing the potential of the periscope within the HARMONI project. Indeed, the periscope accuracy is at the limit of what we want to measure for the HARMONI alignment (10 arcsec and 20 microns for the most critical optics). The remaining challenges serve as opportunities to enhance the periscope’s performance and contribute to future advancements in astronomical instrumentation, particularly in metrology within cryogenic environments.

ACKNOWLEDGMENTS

The CRAL IFU team thanks CNRS/INSU, University Claude-Bernard Lyon I, and LIO for their strong support to the HARMONI project. All members of the HARMONI project office and lead engineers are thanked for their valuable contribution. Finally, we would like to thank Jérémie Bertrand, Lynn Sader and Thomas Barbaire, who worked on the PIC during their internship.

REFERENCES

- [1] Thatte, N. A. et al., “HARMONI: first light spectroscopy for the ELT: instrument final design and quantitative performance predictions,” in [*Ground-based and Airborne Instrumentation for Astronomy VIII*], Evans, C. J., Bryant, J. J., and Motohara, K., eds., **11447**, 114471W, International Society for Optics and Photonics, SPIE (2020).
- [2] Thatte, N. A. et al., “HARMONI at ELT: overview of the capabilities and expected performance of the ELT’s first light, adaptive optics assisted integral field spectrograph.,” in [*Ground-based and Airborne Instrumentation for Astronomy IX*], Evans, C. J., Bryant, J. J., and Motohara, K., eds., **12184**, 1218420, International Society for Optics and Photonics, SPIE (2022).
- [3] Loupías, M. et al., “HARMONI - first light spectroscopy for the ELT: final design of the integral field unit,” in [*Advances in Optical and Mechanical Technologies for Telescopes and Instrumentation IV*], Navarro, R. and Geyl, R., eds., **11451**, 1145138, International Society for Optics and Photonics, SPIE (2020).
- [4] Guibert, M. et al., “HARMONI ELT instrument: integral field unit cryogenic engineering models results,” in [*Advances in Optical and Mechanical Technologies for Telescopes and Instrumentation V*], Navarro, R. and Geyl, R., eds., **12188**, 121881H, International Society for Optics and Photonics, SPIE (2022).
- [5] Bentley, J. and Olson, C., [*Field Guide to Lens Design*], SPIE (12 2012).
- [6] Laurent, F., Boudon, D., Kosmalski, J., Loupías, M., Raffault, G., Remillieux, A., Thatte, N., Bryson, I., Schnetler, H., Clarke, F., and Tecza, M., “ELT HARMONI: image slicer preliminary design,” in [*Ground-based and Airborne Instrumentation for Astronomy VII*], Evans, C. J., Simard, L., and Takami, H., eds., **10702**, 1070296, International Society for Optics and Photonics, SPIE (2018).